14th Czech and Slovak Conference on Magnetism, Košice, Slovakia, July 6–9, 2010

Magnetocaloric Effect in Nanostructured Pr_2Fe_{17} and Nd_2Fe_{17} Synthesized by High-Energy Ball-Milling

P. Alvarez[a], J. Sánchez-Marcos[b], J.L. Sanchez Llamazares[c], V. Franco[d], M. Reiffers[e], J.A. Blanco[a] and P. Gorria[a]

[a]Departamento de Física, Universidad de Oviedo, Calvo Sotelo, s/n, 33007 Oviedo, Spain

[b]Instituto de Ciencia de Materiales de Madrid, CSIC, Cantoblanco, 28049 Madrid, Spain

[c]Instituto Potosino de Investigación Científica y Tecnológica, Camino a la Presa San José 2055, Col. Lomas 4[a], San Luis Potosí, S.L.P. 78216, Mexico

[d]Departamento de Física de la Materia Condensada, ICMSE-CSIC, Universidad de Sevilla P.O. Box 1065, 41080 Sevilla, Spain

[e]Institute of Experimental Physics, Watsonova 47, SK-04001 Košice, Slovakia

Nanocrystalline Pr_2Fe_{17} and Nd_2Fe_{17} powders with rhombohedral Th_2Zn_{17}-type crystal structure and average particle sizes around 20 nm have been obtained by high-energy ball milling. While the bulk alloys show a well-defined and sharp drop in the low-field magnetization curve at the Curie temperature, $T_C = 285$ K (Pr) and 335 K (Nd), the ball-milled samples exhibit a substantial broadening of the ferro-to-paramagnetic transition due to a considerable augmentation of the disordered inter-grain boundaries. The latter results in an increase of more than 25% in the values of the full width at half maximum of the temperature dependence of the magnetic entropy change maintaining almost unchanged the relative cooling power.

PACS numbers: 61.05.cp, 75.50.Tt, 75.30.Kz

1. Introduction

R_2Fe_{17} intermetallic compounds (R = rare earth, Y) are considered very attractive systems for studying competing $3d$–$4f$ magnetic interactions [1]. Among these alloys, Pr_2Fe_{17} and Nd_2Fe_{17} exhibit ferromagnetic order with relatively high values for the saturation magnetization, being close to $\mu \approx 40\ \mu_B$/f.u. at $T = 0$ K, and the Curie temperatures, around room temperature [1]. Both compounds crystallize in the rhombohedral Th_2Zn_{17}-type crystal structure (space group $R\bar{3}m$) with Fe atoms occupying four different sites (6c, 9d, 18f and 18 h in the Wyckoff notation) and a unique 6c site is occupied by the rare-earth [2, 3]. The discovery of a moderate magnetocaloric effect in some R_2Fe_{17} alloys around room temperature, together with their comparatively low-cost processing compared with Gd-based alloys, has renewed the interest in these compounds [4, 5]. High-energy ball-milling (HEBM) is a technique extensively used to modify the microstructure and/or crystal structure of the materials with the consequent effect on their physical properties [6]. We report here on the microstructural, morphological and magnetic changes induced by HEBM on arc-melted R_2Fe_{17} ingots (R = Pr, Nd).

The bulk and 10 h milled powders of Pr_2Fe_{17} and Nd_2Fe_{17} compositions (hereafter ball milled and bulk samples will be referred as Pr(Nd)-BM and Pr(Nd)-Bulk, respectively) were prepared following the process described in [2, 3]. Magnetic entropy change, ΔS_M, was determined as a function of T and H through numerical integration of the isothermally measured $M(H)$ curves up to $\mu_0 H = 1.5$ T, by means of the Maxwell relation

$$\Delta S_M(T,H) = S_M(T,H) - S_M(T,0) = \int_0^H \left(\frac{\partial M}{\partial T}\right)_H \mathrm{d}H\,. \quad (1)$$

Relative cooling power was calculated as

$$\mathrm{RCP}(H) = |\Delta S_M(H)|^{\max} \times \delta T_{\mathrm{FWHM}}(H)\,, \quad (2)$$

where δT_{FWHM} is the full width at half maximum of $|\Delta S_M|$ curve.

2. Results and discussion

Powder morphology of both Pr_2Fe_{17} and Nd_2Fe_{17} ball-milled during 10 h is shown in Fig. 1. SEM micrographs suggest that the powders consist of agglomerated macroscopic grains with irregular shapes, rounded borders and sizes mostly in between 0.5 and 10 μm. Higher magnification micrographs revealed that the grains are close-packed assemblies of smaller, flaky or laminar-like entities. Transmission electron microscopy (TEM) study of the microstructure of these grains at the nanometer length-scale (Fig. 1b and d) showed that the histogram

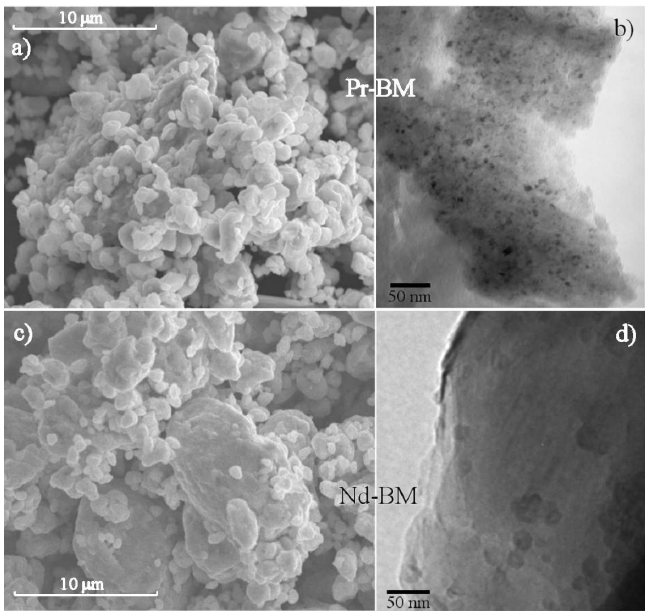

Fig. 1. (a) and (b) SEM and TEM images of Pr_2Fe_{17} BM-10 h alloy. (c) and (d) SEM and TEM images of Nd_2Fe_{17} BM-10 h alloy.

corresponding to the nanoparticle size of a large number of individual particles (> 500 in each compound) follows a log–normal distribution, giving an average size, $\langle\tau\rangle_{\mathrm{TEM}}$, of 23(1) nm for Pr-BM and 17(1) nm for Nd-BM, with a standard deviation $\sigma = 6(1)$ nm in both cases.

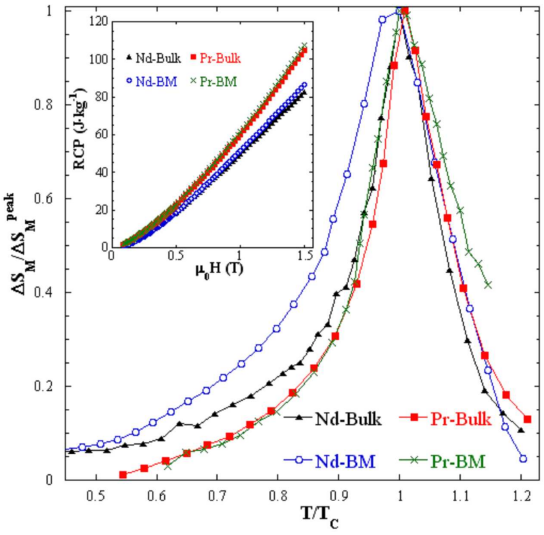

Fig. 2. Normalized magnetic entropy change vs. reduced temperature T/T_{C}. Lines are guides for the eyes. Inset shows the magnetic field dependence of the RCP values for the studied alloys.

That confirms the dramatic mechanically driven nanostructure formation by milling. The analysis of the full-profile X-ray powder diffraction reveals two main characteristics. Firstly, the crystal structure remains unaltered after the HEBM process, with cell parameters (a and c) slightly larger (less than 0.5% in both cases) than those of the bulks (cf. Table).

TABLE

Cell parameters, Curie temperatures and magnetocaloric parameters under an applied magnetic field of $\mu_0 H = 1.5$ T, for both bulk and BM Pr_2Fe_{17} and Nd_2Fe_{17} compounds. Crystal structure was studied by means of X-ray powder diffraction at room temperature.

Sample	a [Å]	c [Å]	T_{C} [K]	$\lvert\Delta S_M\rvert$ [J kg^{-1} K^{-1}]	δT_{FWHM} [K]	RCP [J kg^{-1}]
Pr-Bulk	8.585	12.466	285(2)	2.6	40	105
Pr-BM	8.588	12.470	292(10)	2.1	51	107
Nd-Bulk	8.582	12.462	339(2)	1.7	50	82
Nd-BM	8.586	12.463	340(10)	1.2	72	87

Secondly, a reduction of the peak intensities together with a peak broadening in the patterns corresponding to the BM-10 h samples is observed. The whole profile analysis of the XRD pattern gives an average grain size, $\langle\tau\rangle_{\mathrm{Diff}}$, of 20(2) nm (Pr) and 24(3) (Nd), in reasonable agreement with those estimated from TEM images. Bulk samples do not show any broadening of their peaks with respect to the instrumental line width, which indicates a minimum average grain size of at least 0.1 μm.

The $M(T)$ curves measured under low H reveal that the ferro-to-paramagnetic transition becomes less well-defined after the mechanical treatment, thus suggesting the existence of a broad distribution of T_{C}. The latter is a consequence of the induced structural disorder and the slightly different local environments of the atoms at the grain boundaries [3, 7]. Normalized magnetic entropy change to its maximum value vs. T/T_{C} is depicted in Fig. 2. It is worth noting that the maximum values of

$|\Delta S_M|$ occurs at $T \approx T_C$. The lack of a sharp drop in the $M(T)$ curve at T_C after the HEBM process causes an increase of the width of $\Delta S_M(T)$ and a decrease of the peak value (cf. Table) for all the applied magnetic fields. Nevertheless, the increase of 28 and 44% (for R = Pr and Nd, respectively) in δT_{FWHM} due to the broadening of the $\Delta S_M(T)$ curve after milling, leads to similar RCP values.

3. Conclusion

In summary, the mechanical process generates severe changes in the morphology of the R_2Fe_{17} (R = rare earth) compounds, and entails the reduction of the grain size to the nanometric length scale. These changes are responsible for the modifications in the magnetic behavior, where the main feature is a less well-defined value of T_C, and therefore, the reduction of the magnetic entropy peak is compensated by an enlargement of the temperature span of the peak, giving rise to similar values of the RCP.

Acknowledgments

Financial support from FEDER and Spanish MICINN (projects No. MAT2008-06542-C04-03 & MAT2007--65227), from the PAI of the Regional Government of Andalucía (project No. P06-FQM-01823) and from the Slovak grant agency VEGA 2/0007/09, APVV-VVCE--0058-07 and CLTP-CEX-SAS is acknowledged. P.A. and J.S.M. are grateful for Ph.D. (FICyT) and Juan de la Cierva (MICINN) contracts, respectively. We thank ILL and CRG-D1B for allocating neutron beam time.

References

[1] K.H.J. Buschow, *Rep. Prog. Phys.* **40**, 1179 (1977).

[2] P. Alvarez, J.L Sánchez Llamazares, M.J. Pérez, B. Hernando, J.D. Santos, J. Sánchez-Marcos, J.A. Blanco, P. Gorria, *J. Non-Cryst. Solids* **354**, 5172 (2008).

[3] P. Gorria, P. Alvarez, J. Sánchez-Marcos, J.L Sánchez Llamazares, M.J. Pérez, J.A. Blanco, *Acta Mater.* **57**, 1724 (2009).

[4] P. Gorria, J.L. Sánchez-Llamazares, P. Alvarez, M.J. Pérez, J. Sánchez-Marcos, J.A. Blanco, *J. Phys. D, Appl. Phys.* **41**, 192003 (2008).

[5] P. Álvarez, P. Gorria, V. Franco, J. Sánchez-Marcos, M.J. Pérez, J.L. Sánchez Llamazares, I. Puente Orench, J.A. Blanco, *J. Phys., Condens. Matter* **22**, 216005 (2010).

[6] P. Gorria, D. Martínez-Blanco, M.J. Pérez, J.A. Blanco, A. Hernando, M.A. Laguna-Marco, D. Haskel, N. Souza-Neto, R.I. Smith, W.G. Marshall, G. Garbarino, M. Mezouar, A. Fernández-Martínez, J. Chaboy, L. Fernandez Barquín, J.A. Rodriguez Castrilló n, M. Moldovan, J.I. García Alonso, J. Zhang, A. Llobet, J.S. Jiang, *Phys. Rev. B* **80**, 064421 (2009).

[7] A. Hernando, I. Navarro, P. Gorria, *Phys. Rev. B* **51**, 3281 (1995).